

Supporting Information

Flexible, Stretchable, and Rechargeable Fiber-Shaped Zinc–Air Battery Based on Cross-Stacked Carbon Nanotube Sheets

Yifan Xu, Ye Zhang, Ziyang Guo, Jing Ren, Yonggang Wang, and Huisheng Peng**

anie_201508848_sm_miscellaneous_information.pdf

Supporting Information

Experimental Section

The structures were characterized by scanning electron microscopy (SEM, Hitachi FE-SEM S-4800 operated at 1 kV) and transmission electron microscopy (TEM, JEOL JEM-2100F operated at 200 kV). Powder analysis was performed by an X-ray diffractometer (XRD, Bruker AXS D8). The photograph was taken by a camera (Nikon, J1). The electrochemical performances were measured at an Arbin electrochemical station (MSTAT-5 V/10 mA/16Ch). The discharging performances under bending and stretching were measured with an electrochemical work station (CHI 660D). Two stainless steel plates were inserted vertically into the hydrogel polymer electrolyte face to face with a distance of 1.5 cm to measure the ionic conductivity of the electrolyte through an electrochemical work station (CHI 660D). All electrochemical measurements were conducted in ambient atmosphere at room temperature ($\sim 25^{\circ}\text{C}$). The current density was calculated from the mass of the CNT sheet air electrode or the surface area of the air electrode. The energy and power densities of the fiber-shaped Zn-air battery were calculated by the volume of the whole device.

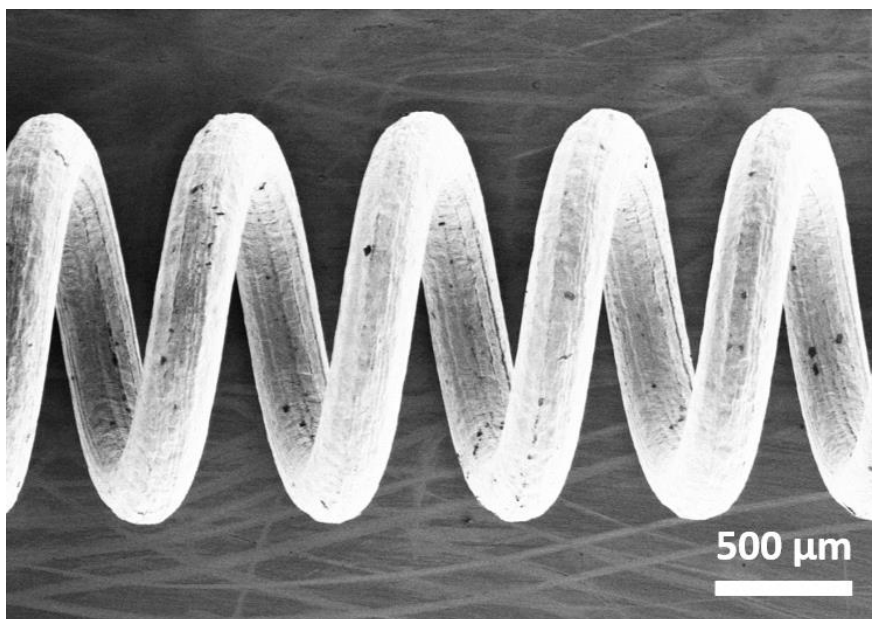


Figure S1. SEM image of a zinc spring.

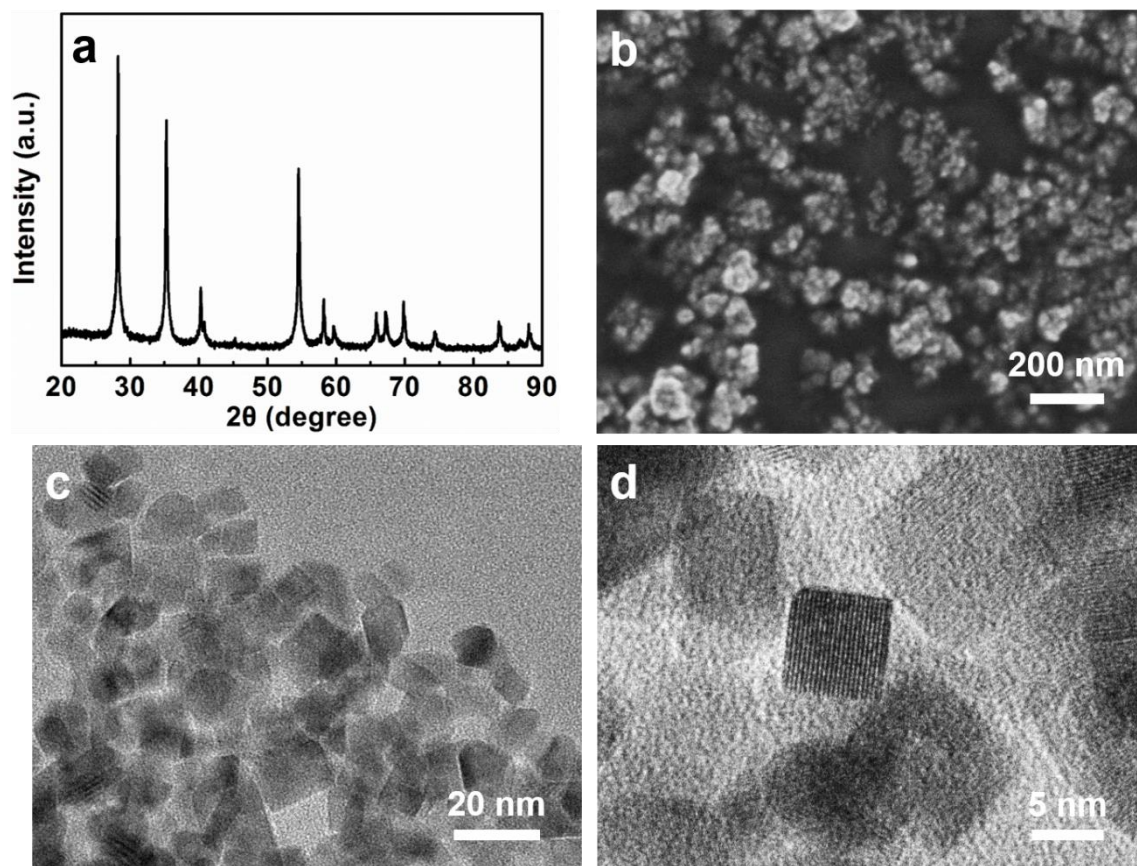


Figure S2. Structure characterizations of the RuO₂ hydrate catalyst by XRD (a), SEM (b) and TEM (c, d).

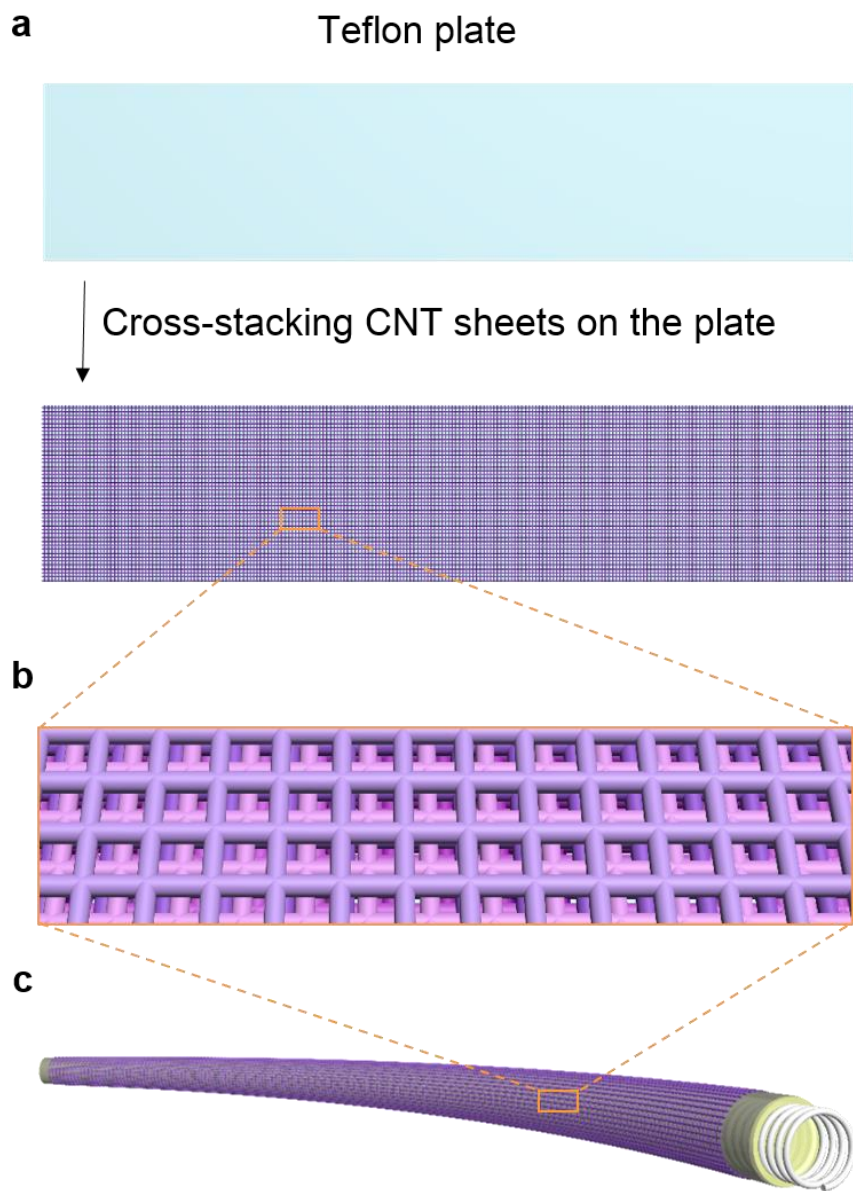


Figure S3. Schematic illustrations to the preparation and characterization of the CNT sheet air electrode. **a)** Cross-stacking the CNT sheets layer by layer on a Teflon plate. **b)** Enlarged view of **a**. **c)** Side view of the fiber-shaped Zn-air battery.

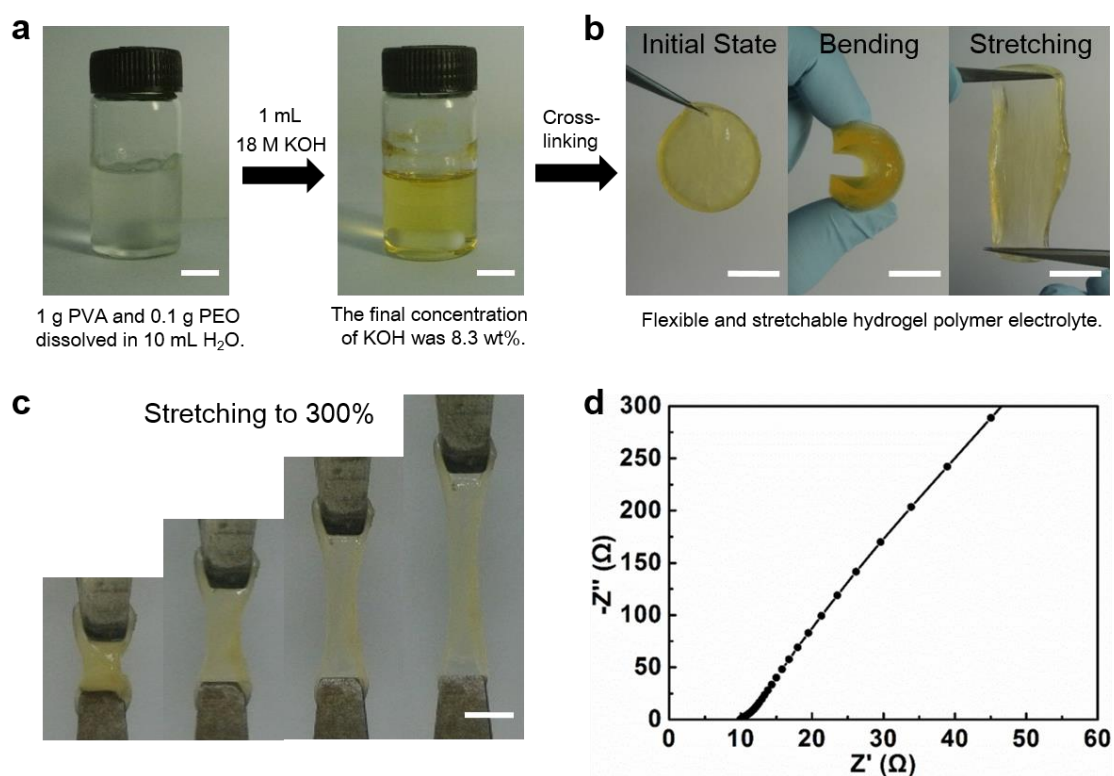


Figure S4. Preparation and characterizations of hydrogel polymer electrolyte. **a)** Photographs of synthetic process of hydrogel polymer electrolyte solution, scale bar: 1 cm. **b)** Photographs of free-standing hydrogel polymer electrolyte after crosslinking, scale bar: 1 cm. **c)** Photographs of hydrogel polymer electrolyte in a stretching process up to 300%, scale bar: 0.5 cm. **d)** Alternating current (AC) impedance spectra of the hydrogel polymer electrolyte at the frequency range from 1000 kHz to 0.01 Hz.

The ionic conductivity of hydrogel polymer electrolyte was calculated by ohmic resistance from AC impedance spectra. The equation can be expressed by $\sigma = l/(R \times A)$, where σ is ionic conductivity, and l , R and A represent the thickness, the resistance, and the area of hydrogel polymer electrolyte between the two stainless plate, respectively. The resistance of the hydrogel electrolyte was 10 Ω , and the thickness and area of the electrolyte were 1.5 cm and 0.5 cm², respectively. The conductivity of the KOH-based hydrogel polymer electrolyte (concentration of 8.3 wt%) was 0.3 S cm⁻¹.

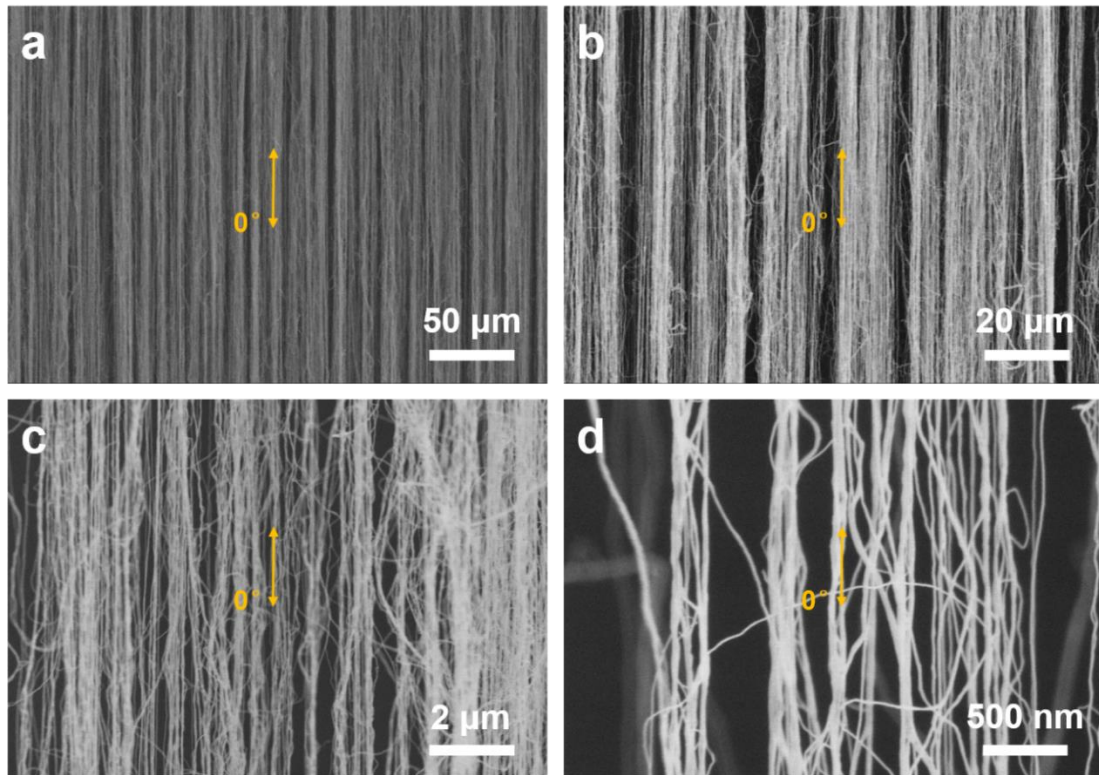


Figure S5. SEM images of aligned CNT sheet air electrode at different magnifications. The CNT sheets were stacked along the aligned direction.

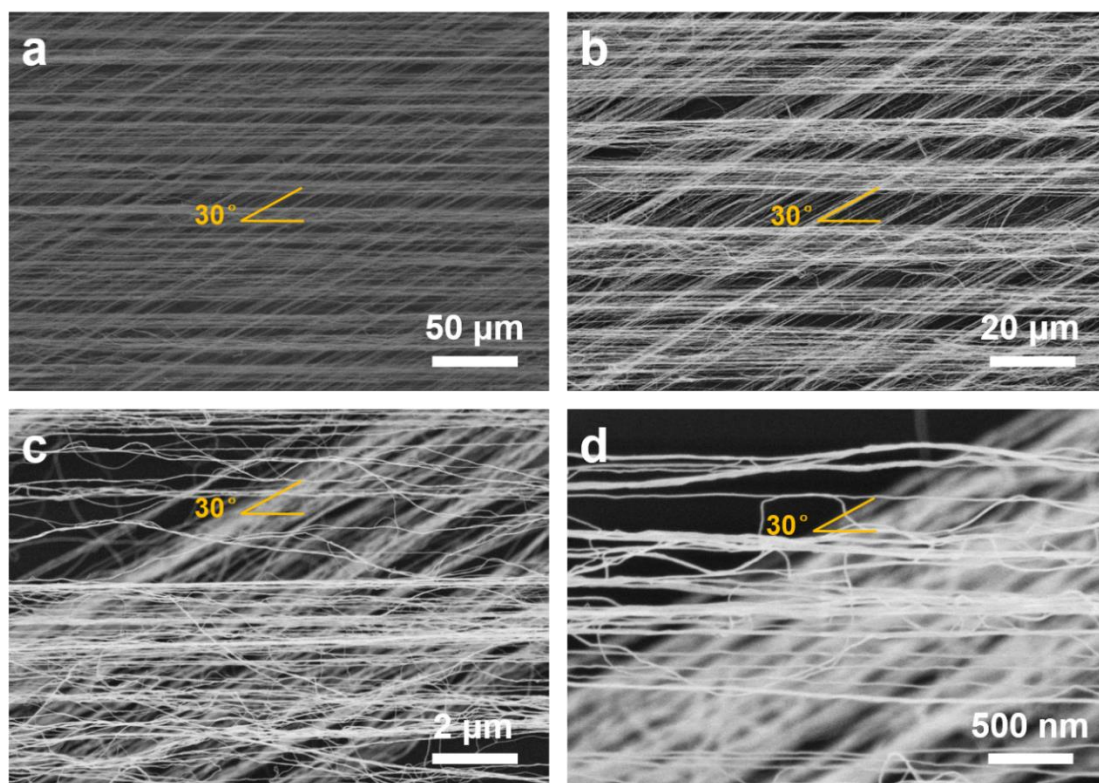


Figure S6. SEM images of aligned CNT sheet air electrode at different magnifications. The CNT sheets were cross-stacked with an angle of 30 °.

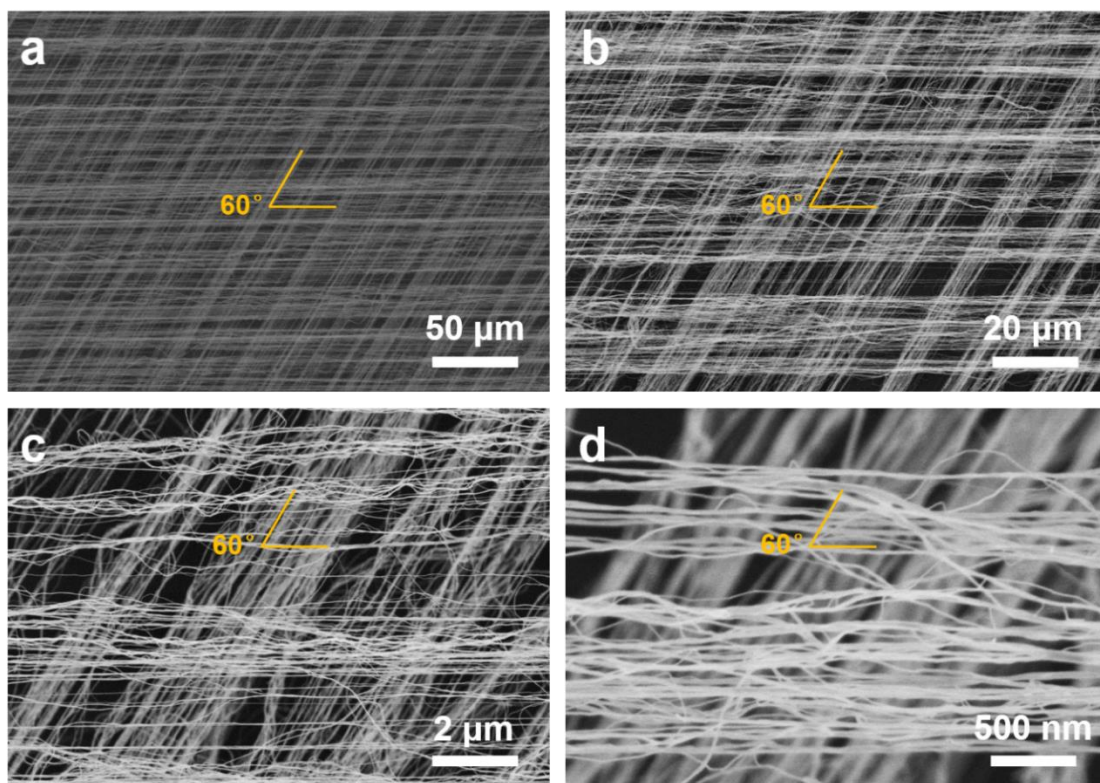


Figure S7. SEM images of aligned CNT sheet air electrode at different magnifications. The CNT sheets were cross-stacked with an angle of 60 °.

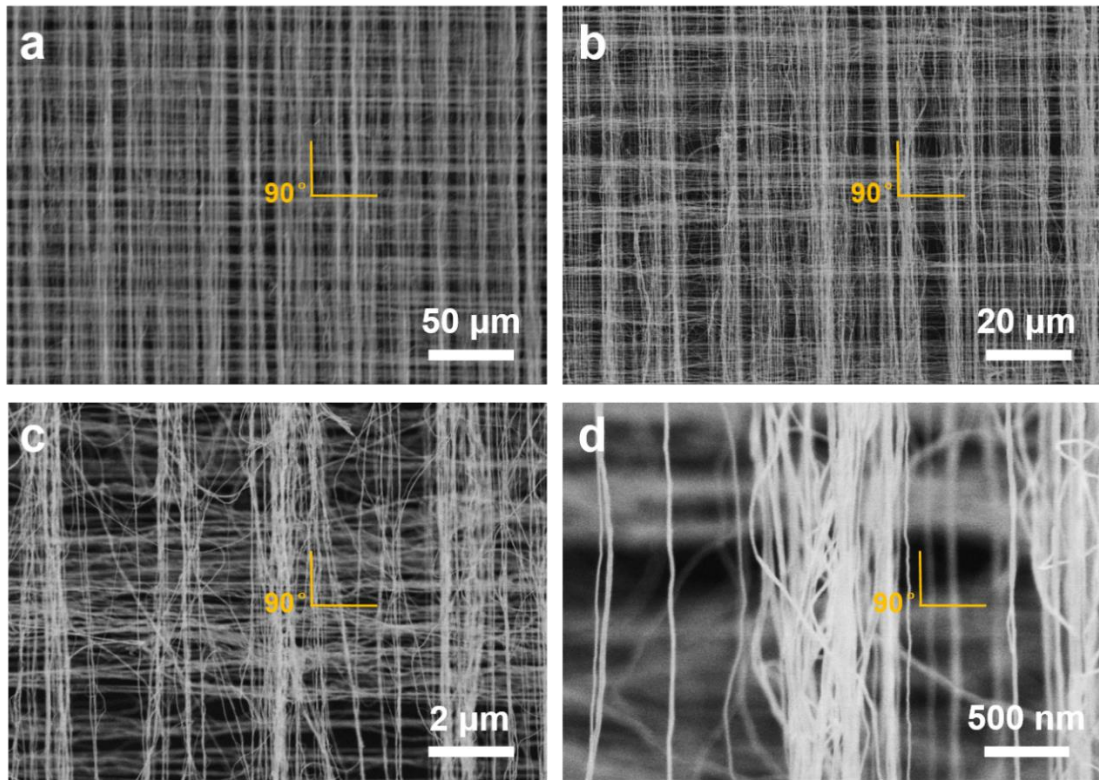


Figure S8. SEM images of aligned CNT sheet air electrode at different magnifications. The CNT sheets were cross-stacked with an angle of 90 °.

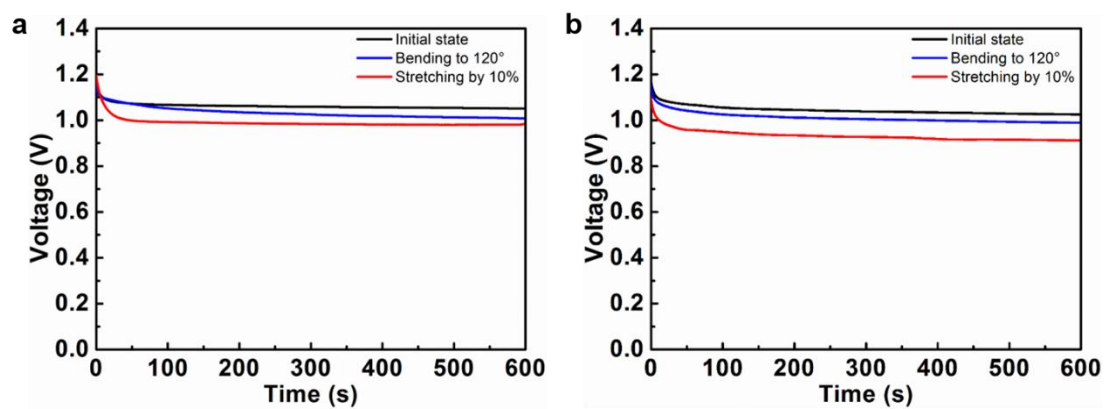


Figure S9. Discharge curves of the fiber-shaped Zn-air battery with a cross-stacking angles of 60° at a current density of 1 A g^{-1} . It was investigated at the initial state and under bending and stretching for Methods A (**a**) and B (**b**). The length of the battery was 1 cm.

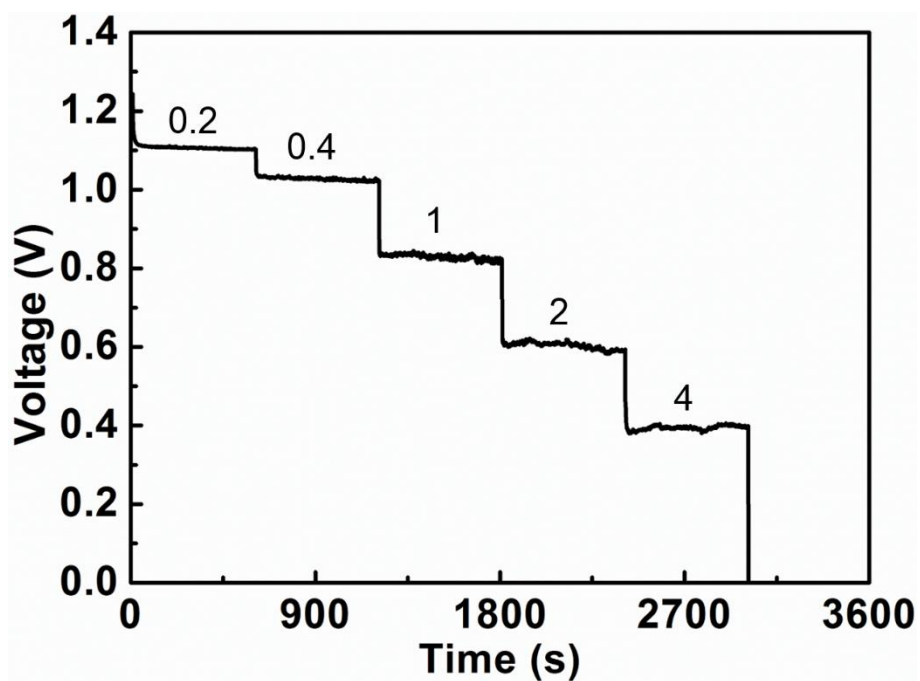


Figure S10. Discharge curves of fiber-shaped Zn-air batteries based on randomly dispersed CNT film air cathode at various current densities. The unit of the current density was A g⁻¹, and the length of the battery was 1 cm.

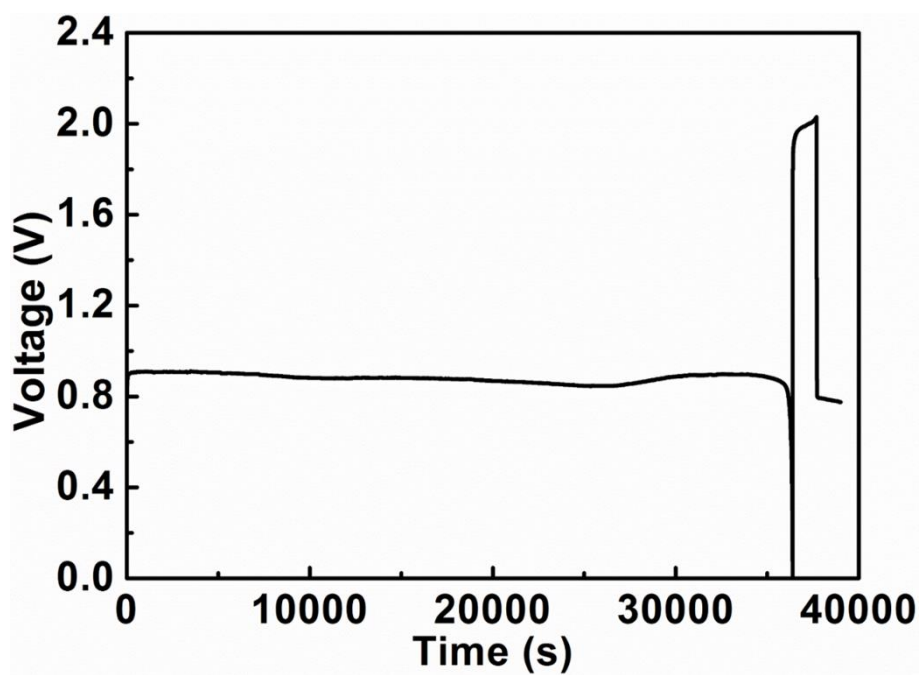


Figure S11. Discharge-charge curve of a fiber-shaped Zn-air battery which was fully discharged at a current density of 2 A g^{-1} , charged at a current density of 2 A g^{-1} , and then discharged again at 2 A g^{-1} . The length of the battery was 2 cm.

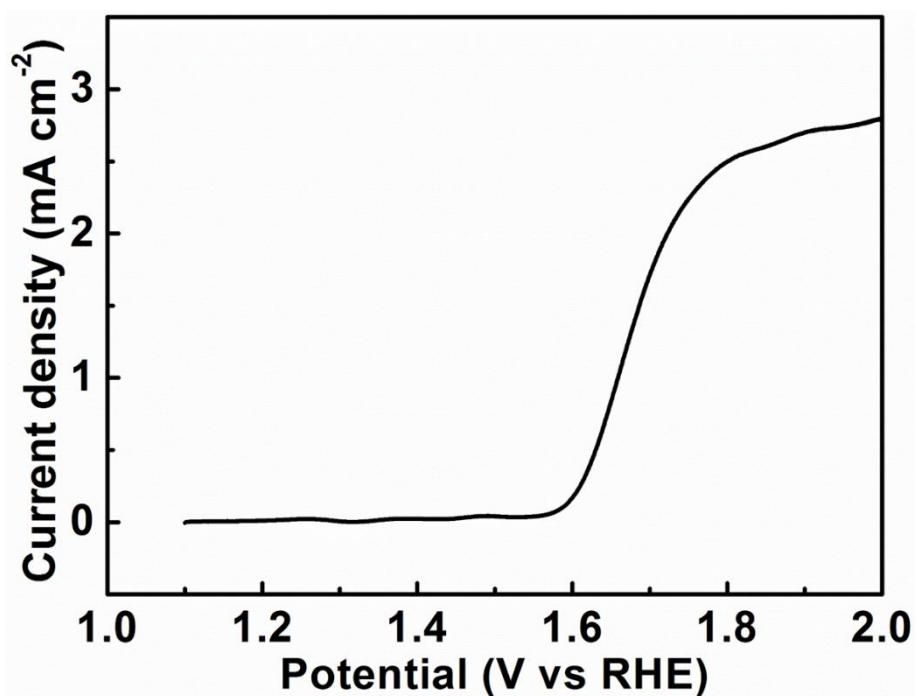


Figure S12. Linear scan voltammogram curves of the oxygen evolution reaction (OER) on RuO₂ hydrate. The potential sweeping rate was 5 mV/s and the electrolyte was 0.1 M KOH solution.

The potential measured against an Hg₂Cl₂/Hg electrode was converted to potential vs RHE according to $E_{\text{vs RHE}} = E_{\text{vs Hg}_2\text{Cl}_2/\text{Hg}} + 0.0591 \text{ pH} + E_{\phi\text{Hg}_2\text{Cl}_2/\text{Hg}}$.

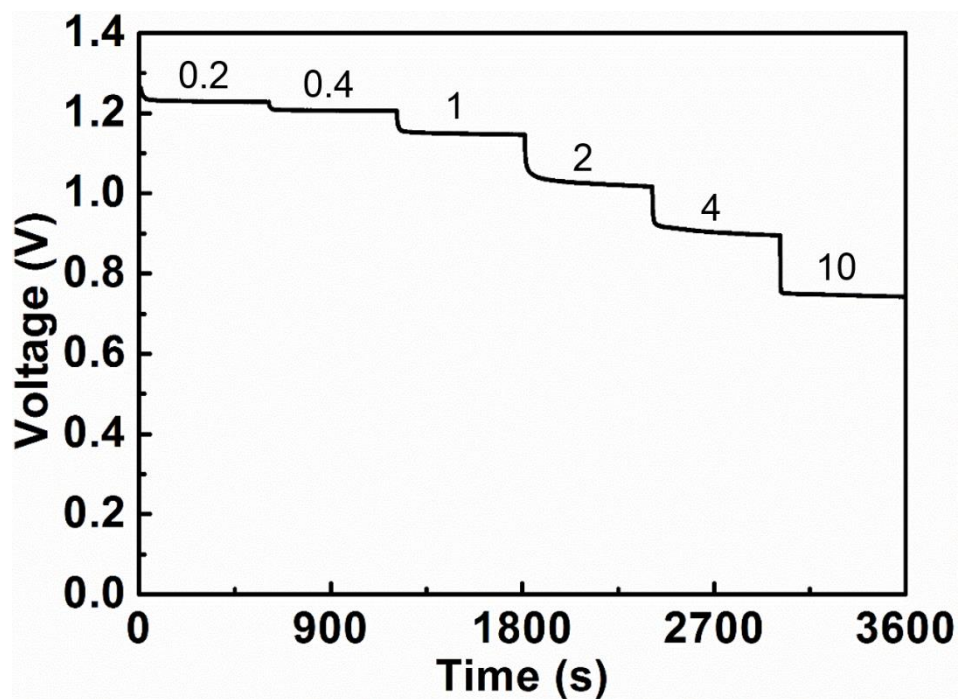


Figure S13. Discharge curve of a fiber-shaped Zn-air battery based on CNT sheet air cathode without the RuO₂ catalyst layer at various current densities. The unit of the current density was A g⁻¹.

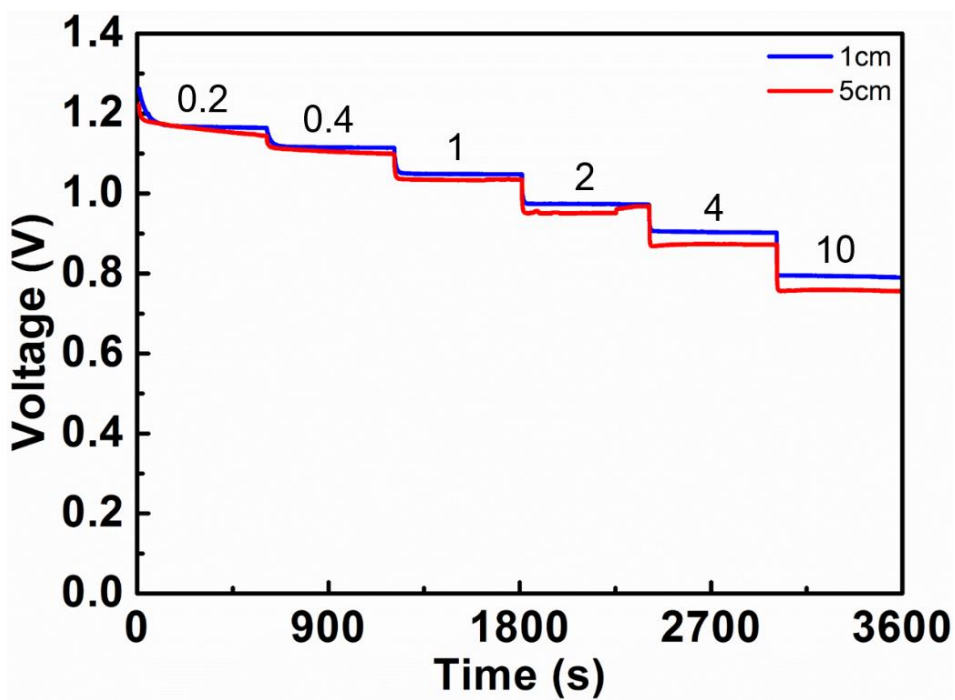


Figure S14. Discharge curves of a fiber-shaped Zn-air battery based on CNT sheet air cathode at various current densities. The unit of the current density was A g⁻¹.